

OPEN ACCESS

## Binder Influence on Rheological Impedance and Graphite Anode Properties

To cite this article: Noah Keim *et al* 2025 *J. Electrochem. Soc.* **172** 090519

View the [article online](#) for updates and enhancements.

### You may also like

- [Understanding the Cathodic Overpotential in  \$\text{LiMn}\_2\text{O}\_4\$  Electrodes for Lithium Recovery from Brines in a Continuous Flow-by Electrochemical Reactor](#)  
Clara Roggerone, Fabio La Mantia, Julia Kowal et al.
- [Understanding Lithium Deposition in Lithium-Ion Batteries: The Link between Impedance Results and Electrochemical Behavior](#)  
Andrea Kinberger, Tom R  ther, Leonard Jahn et al.
- [Microstructure-Tuned Hydrogen Embrittlement in 7050 Aluminum Alloy: Combined Impedance Analysis and Advanced Characterization](#)  
Mingyang Wang, Yuanyuan Ji, Digby D. Macdonald et al.

## ECC-Opto-10 Optical Battery Test Cell: Visualize the Processes Inside Your Battery!

**EL-CELL<sup>®</sup>**  
electrochemical test equipment

### ✓ Battery Test Cell for Optical Characterization

Designed for light microscopy, Raman spectroscopy and XRD.

### ✓ Optimized, Low Profile Cell Design (Device Height 21.5 mm)

Low cell height for high compatibility, fits on standard samples stages.

### ✓ High Cycling Stability and Easy Handling

Dedicated sample holders for different electrode arrangements included!

### ✓ Cell Lids with Different Openings and Window Materials Available



Scan me!

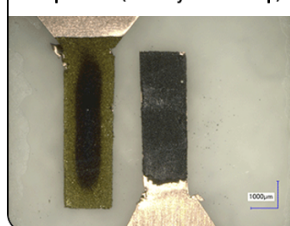
#### Contact us:

+49 40 79012-734

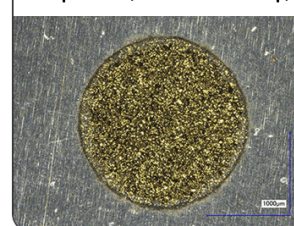
[sales@el-cell.com](mailto:sales@el-cell.com)

[www.el-cell.com](http://www.el-cell.com)

Sample Test (Side-by-Side Setup)



Sample Test (Face-to-Face Setup)





# Binder Influence on Rheological Impedance and Graphite Anode Properties

Noah Keim,<sup>z</sup>  Ulrike Kaufmann, Andreas Weber,  Mattes Renner, Pirmin Koch, Xuebin Wu, Helmut Ehrenberg, and Werner Bauer 

Karlsruhe Institute of Technology, Institute for Applied Materials, Karlsruhe, 76021, Germany

This study investigates the application of simultaneous rheology and impedance spectroscopy (rheo-impedance) for aqueous graphite anode slurries using sodium carboxymethyl cellulose (NaCMC) of varying degrees of substitution (DS), with and without the addition of styrene-butadiene rubber (SBR). Rheo-impedance results reveal that lower DS leads to higher slurry impedance. Interestingly, SBR addition reduces impedance across all formulations, with the strongest effect for DS 0.34, suggesting an unanticipated role of surfactants present in commercial SBR formulations in enhancing carbon additive dispersion. The trends in rheo-impedance are directly translated into the electrical resistance of the anodes, with stronger correlations for less dispersing systems like DS 0.34. However, other anode properties, such as adhesion and water retention, are not affected by changes in rheo-impedance. Electrochemical testing confirms that optimal performance is achieved from a balance between dispersion and water retention, with DS 0.75 showing the best rate capability in this comparison. Thereby, this study demonstrates the potential of rheo-impedance to help better understand electrically relevant features of the slurry and carbon dispersion without the need for coating. © 2025 The Author(s). Published on behalf of The Electrochemical Society by IOP Publishing Limited. This is an open access article distributed under the terms of the Creative Commons Attribution 4.0 License (CC BY, <https://creativecommons.org/licenses/by/4.0/>), which permits unrestricted reuse of the work in any medium, provided the original work is properly cited. [DOI: 10.1149/1945-7111/ae0076]



Manuscript submitted July 4, 2025; revised manuscript received August 19, 2025. Published September 11, 2025.

In lithium-ion battery manufacturing, the quality of the electrode slurry is a key factor in achieving uniform coating, good mechanical, as well as electrical properties, and consistent electrochemical performance.<sup>1,2</sup> However, most existing methods for evaluating the electrode quality focus on post-coating analysis and leaving the analysis of the slurry prior to coating largely unexplored.<sup>3,4</sup> This represents a substantial gap, as poor slurry formulation or inhomogeneity in slurries can lead to defects that only become visible after coating. If this occurs, the materials may already be wasted, and adjustments are not possible anymore.<sup>5,6</sup> Rheo-Impedance offers an opportunity for earlier stage investigation methods, which could provide understanding of the slurry properties before coating occurs and therefore be valuable tools for reducing material waste, reducing production errors, and improve yield in large scale electrode manufacturing.

Graphite anodes are commercially manufactured from water-based slurries, using sodium carboxymethyl cellulose (NaCMC) in combination with styrene-butadiene rubber (SBR) as binders.<sup>1,7,8</sup> Especially NaCMC influences the electrode properties, as they are strongly dependent on the polymers molecular weight (MW) and degree of substitution (DS).<sup>9</sup> Both influence the electrode and slurry via the viscosity, influence binder-particle interactions, slurry stability, and thereby impact the electrode performance. Nevertheless, most research regarding NaCMC-based slurries has focused primarily on the impact on the rheology, without investigating if different NaCMC chemistries may affect other critical aspects of the slurry, such as its electrical resistance or carbon-binder domains in the slurry.<sup>5,10</sup> Therefore, even if the slurry viscosity remains in the target ranges, differences in binder chemistry may still impact the final electrode quality in ways that are currently undetected during slurry preparation.

Previous investigations on the impact of NaCMC on the electrodes were largely performed using characterization methods that are limited to the dried state of the final electrode. While contact angle measurements and binder staining provide insights into binder distribution or electrode surface properties, neither can provide insights into the slurry directly.<sup>3,4</sup> This gap can be filled by using rheological impedance analysis, which offers a non-destructive method to explore both the mechanical and electrical properties of the slurry prior to coating.<sup>11</sup> Furthermore, by using a rheo-impedance system embedding both the working and counter electrodes required

for the impedance measurement in the stationary plate, it removes the limitation of other applications. These limitations include complex setups or unstable electrode contact. The instability of the slurry contact usually is caused by slipping of high solid content suspensions in the rheometer setup on the moving plate. This design increases applicability in research. A schematic illustration of the measurement setup is shown in Fig. 1.

This paper elaborates how variations in rheo-impedance due to different polymer properties in NaCMC translate to changes in electrode properties, like electrical resistance, mechanical sturdiness, or water retention. Finally, electrochemical characterization takes place to evaluate changes manifest themselves in the cell due to changes in the anodes.

## Experimental

This work provides a comparison of different anode slurries containing various NaCMCs with varying degrees of substitution (DS). As a NaCMC is usually classified regarding the viscosity, all NaCMCs used had the same viscosity threshold of 2000 mPa s for a 2 wt-% solution in water. The DS of the NaCMC used is 0.34, 0.75 and 1.23. The gel particle content for all NaCMCs used was smaller than 20.<sup>9</sup>

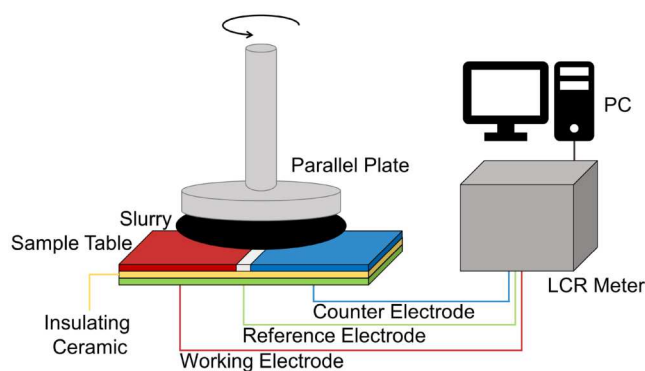
**Materials and mixing.**—If not stated otherwise, the following composition was used for all electrodes, see Table I. The superscript in the abbreviations indicates if SBR is present in the sample or not, while the subscript regards the DS of the NaCMC. For example, a slurry containing a NaCMC with a DS of 0.75 and no SBR would be abbreviated as CMC<sub>0.75</sub><sup>noSBR</sup>.

To manufacture anodes a wet process including slurry coating with a doctor blade was used. The slurry was dispersed using a dissolver (Dispermat CA60, VMA Getzmann, Germany), while placed in a casing that was cooled by 20 °C water. A 2 wt-% NaCMC solution was created before the mixing, by dissolving NaCMC in deionized water. A powder mixture of graphite and CB was then added into the solution and dispersed for 30 min at a tip speed of 5 m s<sup>-1</sup>. At this point, the shear-sensitive SBR was added as well as additional water to adjust the solid content of the slurry to 56 wt-%, and degassed for 5 min at a tip speed of 1 m s<sup>-1</sup>. The anode slurry was finally transferred onto a 10 µm copper foil for roll-to-roll coating (KTFS, Mathis AG, Switzerland) with a doctor blade and a wet-film thickness of 75 µm, resulting in an areal capacity of 2.1 mAh cm<sup>-2</sup>.

<sup>z</sup>E-mail: noah.keim@kit.edu

**Table I.** Anode materials with corresponding manufacturer and the final composition in the dry anode.

Reference	Name	Manufacturer	Final share in anode/wt-%	
			without SBR	with SBR
Graphite (natural)	MechanoCap 1P1	H.C. CARBON, Germany	97.0	96.0
Carbon Black (CB)	C-ENERGY Super C65	Imerys Graphite & Carbon, Switzerland	1.65	1.5
SBR	TRD 2001	JSR Micro, Belgium	—	1.25
NaCMC	Experimental	IFF Speciality Products, Germany	1.35	1.25

**Figure 1.** Schematic illustration of the rheo-impedance setup used with all electrodes in the lower plate, which equals the sample table. The working and counter electrode are separated by an insulating part made of PEEK.

**Rheo-impedance measurements.**—Investigation of the impedance measurements (IM3536, Hioki E.E. Corp., Japan) during shearing of the slurry were performed using a Discovery HR20 (Waters GmbH, Germany).

A plate-plate geometry with a 40 mm diameter and a gap of 500  $\mu\text{m}$  was used. Both the working and the counter electrodes are integrated into the lower plate of the measurement system through a custom design, see Fig. 1. This electrode setup offers an advantage over other designs where one of the electrodes is placed in the upper moving component. By embedding both electrodes into the stationary lower plate, the setup allows for rheological measurements involving large displacements, like tests at high shear rate, in addition to oscillatory tests. This is particularly of interest for slurries with shear-dependent structures, as it enables direct investigation of how microstructural and conductive properties evolve under processing conditions. Rheological impedance spectroscopy was performed of the finished slurry to simultaneously monitor the rheological and electrical properties of the NaCMC-based slurries under shear, with and without SBR. All measurements were carried out at a constant temperature of 20 °C.

The first measurement was a logarithmic shear rate sweep from 0.1  $\text{s}^{-1}$  to 1000  $\text{s}^{-1}$  with ten points per decade. For each shear rate, a dielectric frequency sweep from 100 Hz to 8 MHz was performed. The mentioned shear rates were included in this test, while having a potential of 0.1 V: 0.1  $\text{s}^{-1}$ , 1  $\text{s}^{-1}$ , 10  $\text{s}^{-1}$ , 100  $\text{s}^{-1}$ , and 1000  $\text{s}^{-1}$ . EIS measurement is conducted in less than ten seconds. Therefore, every measured shear rate had a 5 s to allow for equilibrium, followed by a 10 s hold at the shear rate coupled with the EIS measurement. The interval test for the time-dependent effects equaled applying a shear rate of 0.1  $\text{s}^{-1}$ , followed by a high shear rate of 1000  $\text{s}^{-1}$ , and again a low shear rate of 0.1  $\text{s}^{-1}$ . All steps had a set duration of 300 s. The detailed settings for measurement time (5 s + 10 s) are only true for the shear rate sweep. In the interval test, the sample was continuously sheared and every 30 s a (rheological) data point as well as a dielectric frequency sweep was performed.

**Adhesion strength measurements.**—Adhesion strength was measured in a 90° peel-off test. Each test had three 17 mm  $\times$  60 mm samples measured and pressed onto a double-sided adhesive

tape with a load of 0.3 MPa for 10 s to enhance comparability. It was then placed in a ZwickiLine Z2.5/TN (ZwickRoell, Germany), which pulled the current collector foil at 600  $\text{mm min}^{-1}$  while measuring the force needed for separation by a 10 N load cell over a distance of 40 mm, discarding the data from the first and last 10 mm of the sample. The average force was then divided by the width of the sample according to ISO 813:2019, resulting in the adhesion strength in  $\text{N m}^{-1}$ .<sup>12</sup> The standard deviation of the three measurements is displayed as error bars.

**Resistivity measurements.**—Bulk resistivity and interface resistance were determined simultaneously using the DC 4-terminal measurement (RM2610 Electrode Resistance Measurement System, Hioki E.E. Corp., Japan) based on the finite volume method. Five randomly chosen locations were selected for each anode for measurement, which resulted in the standard deviation displayed.

**Residual water determined with Karl Fischer.**—The anodes residual water was determined by Karl Fischer titration, using the Karl Fischer oven.<sup>13</sup> The Karl Fischer titration was carried out in a dry room with a dew point of  $-60$  °C. Electrode sheets were prepared as if used in a cell, i.e. they were densified to a porosity of 50% and dried for 16 h at 120 °C under vacuum conditions. The electrodes were cut into roughly 30 mm  $\times$  100 mm samples, resulting in 180 mg anode material per sample, and put into the prepared vials. The sample chamber was then heated to a temperature of 160 °C for 12 min for the residual water to be extracted. To calculate the mean average and standard deviation three measurements were conducted.

**Electrochemical characterization.**—Electrochemical characterization of the anodes was conducted by using laboratory pouch cell format. All electrodes were densified to a porosity of 50% and dried for 16 h at 120 °C under vacuum conditions before they were assembled in a dry room with a dew point of  $-60$  °C. The cathode consisted of NMC(622) as active material with a mass loading of 12  $\text{mg cm}^{-2}$ . The density of the electrode was constant at 2.7  $\text{g cm}^{-3}$  with a cathode area of 25  $\text{cm}^2$  in the cell. The anode (29  $\text{cm}^2$ ) was slightly overbalanced with an N/P ratio of 1.2. Pouch cells were assembled with the electrodes separated by a separator (33.4  $\text{cm}^2$ , ceramic, SEPARION, Degussa AG, Germany) and filled with electrolyte consisting of EC:DMC (1:1, Vol/Vol) with 1 M of LiPF<sub>6</sub> dissolved (LP30, Sigma-Aldrich, USA). SEPARION is a commercially available ceramic-coated (aluminum oxide) polyethylene terephthalate separator.<sup>14</sup> Before cycling, the pouch cells were stored at 40 °C for a minimum of 16 h to allow for proper electrolyte wetting. To investigate the cycling behavior, the cells were connected to a BaSyTec battery test system (CTS-LAB, BaSyTec, Germany) and stored in a climate chamber at 20 °C. Both formation and cycling were based on the theoretical capacity of the cathode (175  $\text{mAh g}^{-1}$ ). Electrochemical testing began by conducting a discharge rate capability test (0.5/0.5, 1/1, 1/2, 1/3, 1/5 C, constant current (CC) + constant voltage (CV) charge/CC discharge), which was concluded by long-term investigations of 1000 cycles (1 C CC CV charge/3 C CC discharge). The voltage window of the cells was 3.0 V to 4.2 V. Cut-off current for the CV step was set to 0.05 C. Furthermore, two 0.05 C steps were included every 200 cycles to

have insights into reversible and irreversible capacity loss during long-term cycling. For comparability, three laboratory pouch cells were built per sample. Displayed capacities and standard deviation are based on the mean average of those three pouch cells.

## Results and Discussion

**Rheo-impedance of anode slurries.**—Figure 2 compiles the results of the rheo-impedance measurements regarding the slurries containing different NaCMCs, with and without SBR, for a set shear rate of  $10\text{ s}^{-1}$ . All individual results of the rheo-impedance measurements for each slurry are summarized in Fig. A.1. Furthermore, the internal resistance  $R_{\Sigma}$  determined via the impedance was calculated using a linear fit.<sup>15</sup> In short, Laschuk et al. describe the internal resistance  $R_{\Sigma}$  as the sum of the electrical and ionic resistance.<sup>15</sup> The intersection of the different linearized parts of the impedance lead to the determination of  $R_{\Sigma}/3$  which is then calculated accordingly.

The results indicate a trend, where slurries containing lower DS NaCMC exhibit a higher resistance, while higher DS corresponds to lower impedance. This trend is observable for slurries independent of SBR addition. The resistance for slurries containing no SBR decreases from  $111\ \Omega$  for DS 0.34, to  $70.5\ \Omega$  for DS 0.75 to  $53.3\ \Omega$  for a slurry containing NaCMC with DS 1.23. This indicates that the rheo-impedance of anode slurries is dependent on the DS of the NaCMC. These observations are in line with separate findings of Gordon et al.<sup>10</sup> and Weber et al.<sup>4</sup> who reported that NaCMC with lower DS shows increased adsorption to graphite surfaces and lowered affinity to carbon additives in the aqueous slurry. Excessive polymer adsorption or increased preference of the NaCMC for the graphite instead of the carbon additive may interfere with conductive carbon pathways.<sup>4,10,16,17</sup> This results in higher electrical resistance within the slurry, which is consistent with the higher impedance observed for decreasing DS in this study. Slurries containing higher DS NaCMC, on the opposite, reduce interparticle bridging and network formation due to higher electrostatic repulsion between the chains, which lowers impedance.<sup>16,17</sup> This repulsion is therefore leading to more spread out NaCMC polymer chains, changing the distribution of the CB, and thereby decreasing the resistance inside the slurry.

Furthermore, independent of NaCMC polymer properties, the addition of SBR leads to a reduction of the impedance. This outcome was unexpected, as SBR is traditionally not considered a dispersant and rather as an additive for mechanical properties, whereas CMC is recognized for its dispersing capabilities.<sup>7,10,16,18,19</sup> The most pronounced effect of SBR on impedance was observed in the slurry containing NaCMC with a DS of 0.34 decreasing the resistance from  $111\ \Omega$  to  $83.4\ \Omega$ . The observed reduction of the impedance suggests that SBR, or components associated with it, may influence conductive properties of the slurry through mechanisms beyond its primary role as a binder. One possible explanation is the presence of surfactants within commercial SBR latex formulations, which are present to stabilize the latex in the suspension.<sup>3</sup> Those surfactants can adsorb onto the carbon black particles, changing the surface free

energy of the particle, and can reduce agglomeration in the slurry, leading to better conductive networks.<sup>4,20</sup> Especially considering that the impact on the formulation with the NaCMC, which has the lowest affinity towards carbon black, changed the most.

Figure 3 displays the results of the time-dependent rheology test for slurries, which starts at shear rate of  $0.1\text{ s}^{-1}$ , increases to  $1000\text{ s}^{-1}$ , and going back to  $0.1\text{ s}^{-1}$ . Slurries again were prepared with NaCMCs of different DS, as well as with and without SBR.

In these measurements, all slurries showed reversible behavior, except those formulated containing NaCMC with DS 0.34. This indicates that the slurries containing NaCMC with a DS of 0.75 and 1.23 are capable of maintaining or recovering their internal network structure after shear is removed. The irreversible behavior in the CMC<sub>0.34</sub><sup>SBR</sup> system likely stems from intermolecular interactions of the NaCMC being disrupted under shear and is hindered from fully recovering. This behavior is likely attributed to the higher density of hydroxyl groups present in low DS NaCMC, which facilitates stronger intermolecular hydrogen bonding and the creation of fringed micelles, resulting in high viscosities for NaCMCs with a DS of lower than 0.9.<sup>21–25</sup> low DS values show a significant fraction of unsubstituted hydroxyl groups remaining along the cellulose backbone. These groups promote intermolecular hydrogen bonding and limit chain mobility and thereby flexibility of the low DS NaCMC. Furthermore, the hydration of the chains is reduced, as the water molecules are rather localized at few hydrogen bonded regions present rather than forming extended hydration shells at the carboxymethyl moieties of the higher substituted NaCMCs.<sup>4,16,17</sup> While slurries containing DS 0.75 can recover, once these interactions are disrupted under shear for DS 0.34, the lower chain flexibility and lower hydration of the polymer likely hinders the reformation of the initial structure in the time frame investigated.<sup>16</sup> SBR interferes with the formation of the interchain associations even more, thereby impacting the gel-like behavior and reducing the viscosity of the low DS NaCMC slurries.<sup>16,24</sup> It is further reported that the addition of monovalent salts can further limit the interactions and reduce viscosity.<sup>24</sup> Salt in the form of sodium dodecyl sulfate is introduced via SBR. This could be a further reason for the difference in the viscosity for both slurries containing NaCMCs with DS 0.34 and DS 0.75.<sup>3</sup> Nevertheless, while the surfactant is considered a monovalent salt, the properties as surfactant influence could be more impactful regarding the viscosity.

The impedance of the slurries, aside from the discussed differences introduced by the presence of SBR, remained consistent across all time-dependent rheology tests. No significant changes in impedance were observed before or after the application of shear, indicating that the electrical characteristics were largely unaffected by the mechanical strain of the slurry. This stability in measurement results suggests that shear-induced rearrangements did not drastically alter the ionic or electronic conduction pathways. It also indicates that all slurries were already properly mixed and did not show any more agglomerates of carbon additive, independent of the formulation used. The full impedance profiles supporting this conclusion are provided in Fig. A.2.

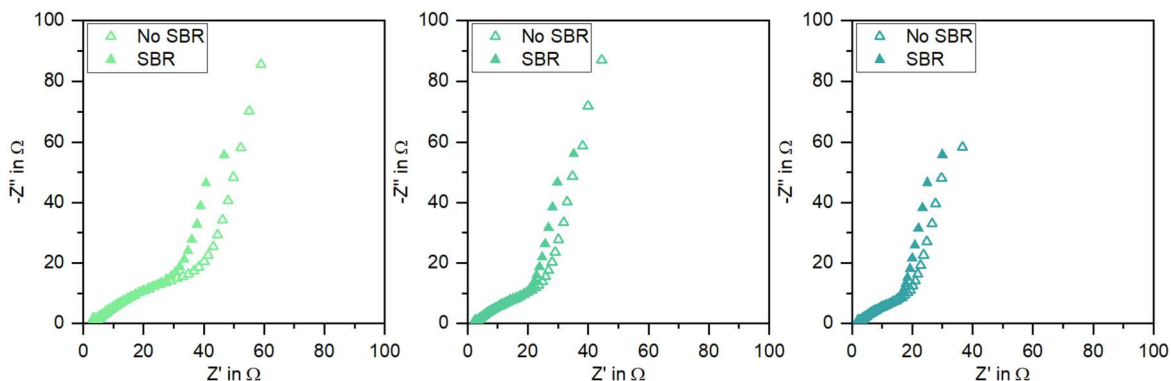


**Figure 2.** Summary of the rheo-impedance measurements for slurries containing NaCMCs with varying DS, with and without SBR at a shear rate of  $10\text{ s}^{-1}$ .



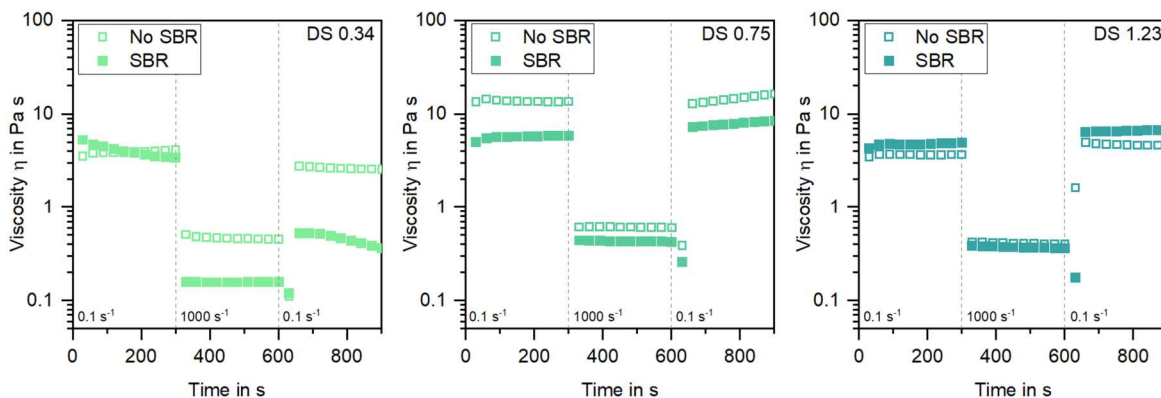


**Figure 3.** Summary of the time-dependent rheology test for slurries containing various NaCMCs with and without SBR.

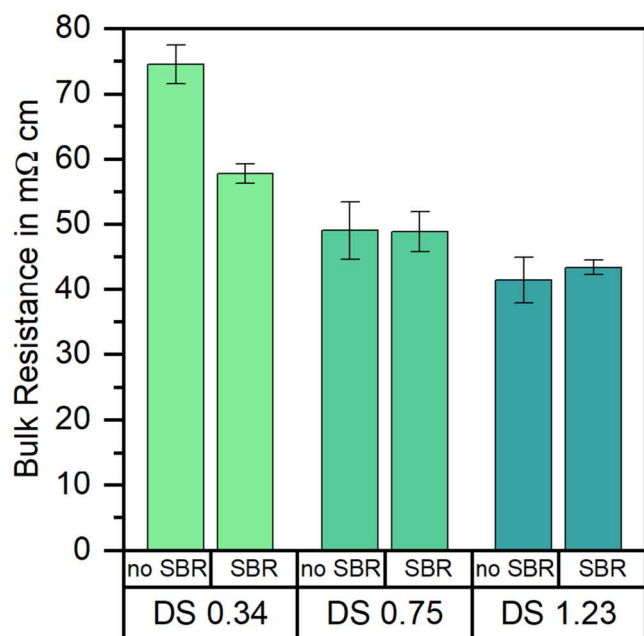


**Figure 4.** Bulk resistance of aqueously processed anodes containing NaCMCs with differing DS and either with or without SBR. In parts reproduced from Ref. 26.

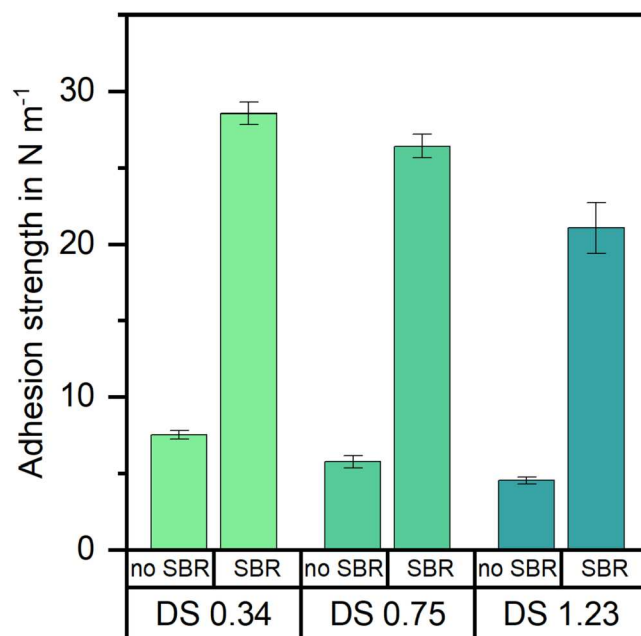


**Figure 5.** Adhesion strength of aqueously processed anodes containing NaCMCs with differing DS and either with or without SBR. In parts reproduced from Ref. 26.

#### Electrode properties and electrochemical characterization.—

Key electrode properties of the anodes include their resistivity and mechanical strength, for which it is of special interest, if the investigations of the rheo-impedance of the anode slurries align with the results of the post-coating anodes.

As shown in Fig. 4, the electrodes formulated with DS 0.34 consistently exhibit the highest bulk resistance, regardless if SBR is present or not. In contrast, anodes produced with NaCMC of DS 0.75 and 1.23 showed lower resistances, with negligible differences between anodes containing SBR or not. This indicates that the influence of SBR on bulk resistance is negligible at higher DS values, while it becomes significant only in the low DS system. These findings align with previous reports, which suggest that increasing the DS leads to better dispersion of the conductive additive during processing.<sup>4,9</sup> Additionally, the trend observed in the bulk resistance aligns well with the results from the earlier rheo-impedance measurements. Only the DS 0.34 slurries showed substantial differences in rheological impedance upon SBR addition, and these differences are now observed in the corresponding electrode resistance as well. This

correlation indicates that the impact visible in the slurry phase, particularly for poorly dispersing systems, in this case DS 0.34, can persist into the dry electrode and directly influence its electrical performance. Furthermore, the relative trends observed in the rheo-impedance are also observed in the bulk resistance. Specifically, samples prepared with DS 0.34 have both the highest impedance and the highest bulk resistance, followed by DS 0.75, while DS 1.23 has the lowest values. This suggests that the dispersion quality can be characterized via rheo-impedance and translates into measurable differences in the electric resistance for the anodes.

In addition to electrical properties, the adhesion strength of the electrodes was evaluated to assess mechanical integrity, see Fig. 5. The results show that electrodes containing NaCMC with a DS of 0.34 exhibit the highest adhesion strength, independent of whether SBR is present or not. Anodes with higher DS (e.g. 0.75 and 1.23) NaCMC display lower adhesion values. This trend aligns with other reports, suggesting that a stronger affinity of the low DS NaCMC towards SBR and the current collector contributes to improved mechanical strength.<sup>4,9,22</sup>

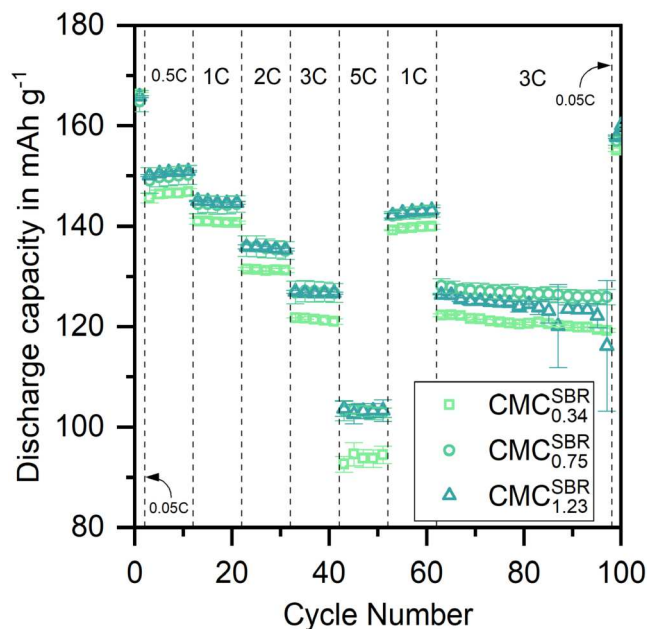


**Figure 6.** Rate test for electrodes containing NaCMC with various DS and SBR. For the sake of visibility, only every second value is shown in the rate test. In parts reproduced from Ref. 26.

The electrodes not containing SBR were not investigated electrochemically, as they showed too little mechanical stability to ensure that no delamination of the anode is occurring during cell manufacturing. Therefore, the rate test displayed in Fig. 6 only contains cell results for anodes that included SBR in their formulation. The results of the rate performance test reveal clear differences between the electrodes prepared with NaCMC of varying degrees of substitution. Electrodes with DS 0.75 showed the best rate capability, followed by DS 1.23 and DS 0.34. These findings are in line with previous reports and further support the conclusion that a balance between low bulk resistance (Fig. 3) and moderate water retention (Fig. A-4) is critical for optimal performance.<sup>4,9</sup> While DS 1.23 benefits from low resistance, its high water retention leads to early signs of cell degradation at higher cycling rates, likely due to increased SEI formation and instability.<sup>27–29</sup> long-term cycling investigations (Fig. A-3) provided no further insights, as DS 1.23 had to be discontinued early, and the degradation behavior of the remaining samples containing either DS 0.34 or DS 0.75 was comparable over extended cycling duration.

## Conclusions

This study highlights the use of rheo-impedance to further expand the characterization of anodes by identifying dispersion-related changes prior to the coating of the anode. Slurries containing low DS NaCMC showed high slurry impedance and high bulk resistance of the dry anode. Both the slurry impedance and bulk resistance of the dry anode decreased for increasing DS, which is connected to better dispersed carbon additive and was observable even before coating. This demonstrates that rheo-impedance can be used as a tool to allow to compare the development of the conductive additive domain formation even before coating. Furthermore, this study revealed that the addition of SBR can unexpectedly help in reducing impedance and thereby electrical resistance of the coating for systems showing insufficient dispersion of the carbon additive, like in case of DS 0.34. For these improvements, surfactant components of SBR are suspected to play a significant role by modifying particle interactions. For practical implications, this means that for poorly dispersing systems, additives like SBR can contribute positively to electrical performance than compared to what is usually assumed. Nevertheless, not all relevant electrode properties are linked to impedance or DS alone. As for example, the mechanical stability was as expected dependent on if SBR as adhesive additive was used or not. Therefore, to evaluate electrochemical performance and mechanical stability, a balanced formulation is required, for which DS 0.75 showed the best compromise between electrical and mechanical properties in this work.

Finally, the demonstrated method opens new possibilities for slurry characterization. Rheo-impedance is simple to implement and has shown consistent correlation with final electrode resistance, enabling early detection of insufficient conductive additive dispersion.

## Acknowledgments

This work contributes to the research performed at CELEST (Center for Electrochemical Energy Storage Ulm Karlsruhe) and Material Research Center for Energy Systems (MZE). During drafting this article Large Language Models were used. While the model was used to aid in ensuring readability, all data-analysis, interpretations, conclusions, and final edits were made by the authors. The authors take full responsibility for the accuracy, validity, and originality of the content presented. The authors thank Dr Roland Bayer and Dr Oliver Petermann (IFF, Inc.) for providing the binders. We also want to thank Dr Lukas Schwab (Waters GmbH) for providing valuable insights into the method of rheo-impedance and fruitful discussion.

## Appendix

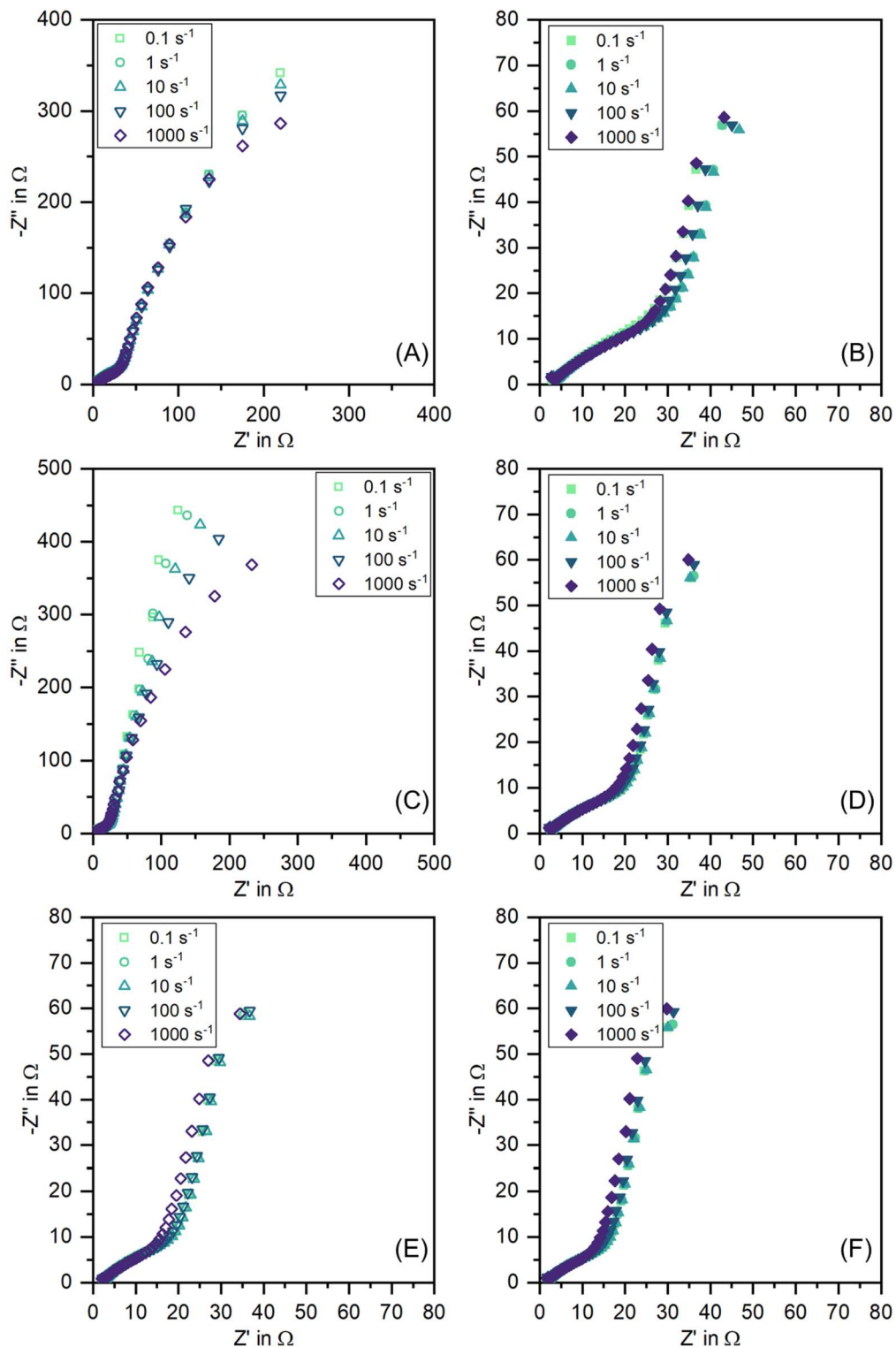


**Figure A-1.** Summary of all EIS measurements for different shear rates. Hollow points indicate a slurry sample, without SBR, while filled points indicate a slurry sample containing SBR. Letters indicate which slurry was measured: (A)  $CMC_{0.34}^{noSBR}$ , (B)  $CMC_{0.34}^{SBR}$ , (C)  $CMC_{0.75}^{noSBR}$ , (D)  $CMC_{0.75}^{SBR}$ , (E)  $CMC_{1.23}^{noSBR}$ , (F)  $CMC_{1.23}^{SBR}$ .

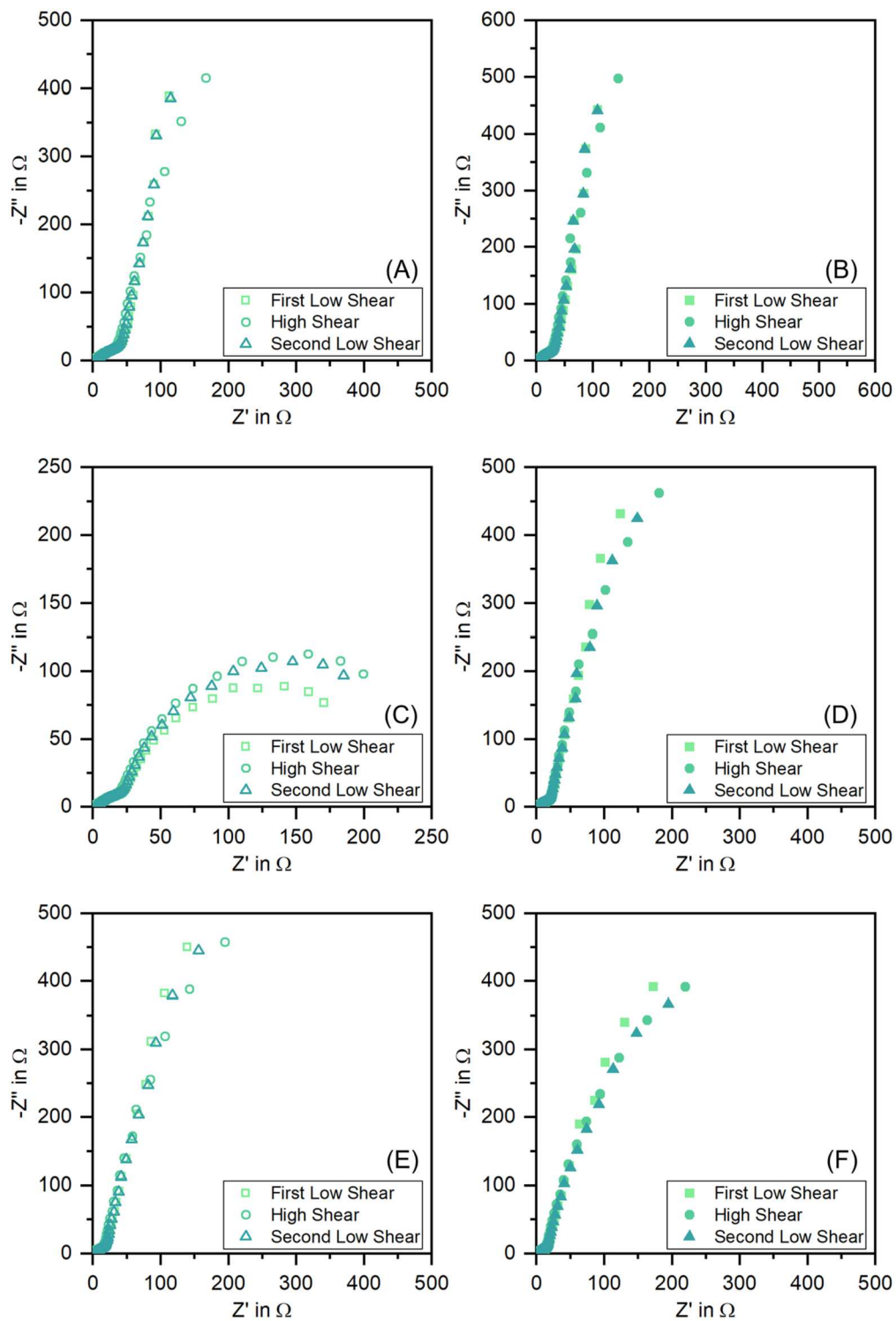


**Figure A-2.** Summary of all EIS measurements for different shear rates during time dependent measurements. Hollow points indicate a slurry sample, without SBR, while filled points indicate a slurry sample containing SBR. Letters indicate which slurry was measured: (A)  $CMC_{0.34}^{noSBR}$ , (B)  $CMC_{0.34}^{SBR}$ , (C)  $CMC_{0.75}^{noSBR}$ , (D)  $CMC_{0.75}^{SBR}$ , (E)  $CMC_{1.23}^{noSBR}$ , (F)  $CMC_{1.23}^{SBR}$ .



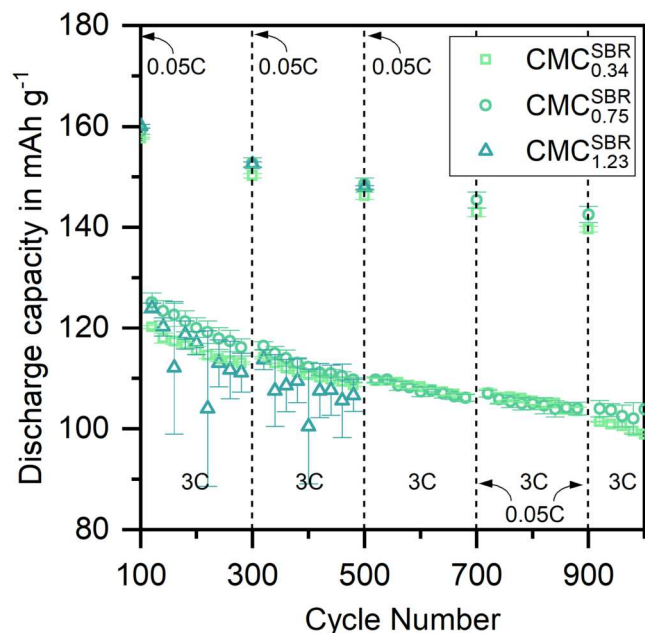


**Figure A-3.** Long-term cell cycling for electrodes containing NaCMC with various DS. Every 200 cycles there are two 0.05 C cycles during long term cycling. For the sake of visibility, only every 20th for the long-term cycling is shown (in part reproduced from Ref. 26).

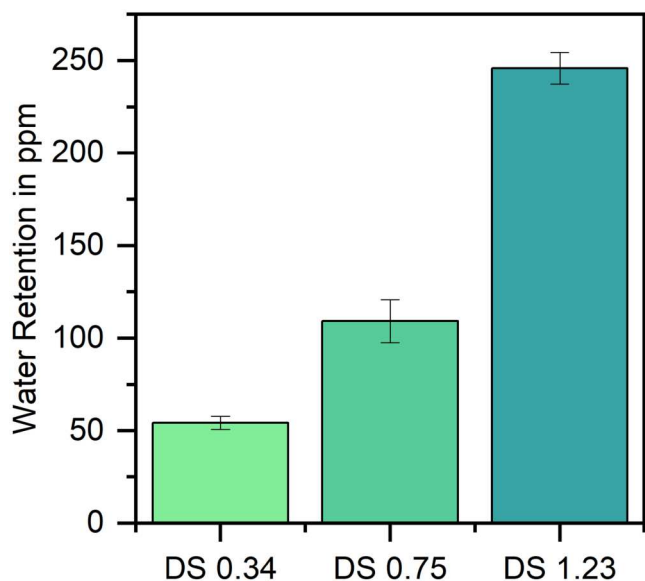


**Figure A-4.** Water retention of anodes containing SBR (in part reproduced from Ref. 4, 26).

#### ORCID

Noah Keim <https://orcid.org/0000-0002-3338-5811>  
 Andreas Weber <https://orcid.org/0009-0008-4104-0961>  
 Werner Bauer <https://orcid.org/0000-0002-5923-2426>

#### References

1. D. Bresser, D. Buchholz, A. Moretti, A. Varzi, and S. Passerini, "Alternative binders for sustainable electrochemical energy storage—the transition to aqueous electrode processing and bio-derived polymers." *Energy Environ. Sci.*, **11**, 3096 (2018).
2. Y. Liu, R. Zhang, J. Wang, and Y. Wang, "Current and future lithium-ion battery manufacturing." *iScience*, **24**, 102332 (2021).

3. N. Keim, A. Weber, M. Müller, D. Burger, W. Bauer, P. Scharfer, W. Schabel, and H. Ehrenberg, "CMC staining method for the visualization of the binder distribution in water-based electrodes with EDS." *ACS Appl. Energy Mater.*, **8**, 4501 (2025).
4. A. Weber, N. Keim, P. Koch, M. Müller, W. Bauer, and H. Ehrenberg, "The impact of binder polarity on the properties of aqueously processed positive and negative electrodes for lithium-ion batteries." *Sci. Rep.*, **15**, 10024 (2025).
5. C. D. Reynolds, H. Walker, A. Mahgoub, E. Adebayo, and E. Kendrick, "Battery electrode slurry rheology and its impact on manufacturing." *Energy Advances*, **4**, 84 (2025).
6. M. Schmitt, "Slot Die Coating of Lithium-Ion Battery Electrodes." *Dissertation*, Karlsruhe Institute of Technology (2016), [10.5445/ksp/1000051733](https://doi.org/10.5445/ksp/1000051733).
7. D. Burger, N. Keim, J. Shabbir, Y. Gao, M. Müller, W. Bauer, A. Hoffmann, P. Scharfer, and W. Schabel, "Simultaneous primer coating for fast drying of battery electrodes." *Energy Technology*, **13**, 2401668 (2025).
8. J.-H. Lee, S. Lee, U. Paik, and Y.-M. Choi, "Aqueous processing of natural graphite particulates for lithium-ion battery anodes and their electrochemical performance." *J. Power Sources*, **147**, 249 (2005).
9. N. Keim, A. Weber, M. Müller, U. Kaufmann, W. Bauer, O. Petermann, R. Bayer, and H. Ehrenberg, "Understanding key NaCMC properties to optimize electrodes and battery performance." *Advanced Energy and Sustainability Research*, **n/a**, 2400364 (2025).
10. R. Gordon, R. Orias, and N. Willenbacher, "Effect of carboxymethyl cellulose on the flow behavior of lithium-ion battery anode slurries and the electrical as well as mechanical properties of corresponding dry layers." *J. Mater. Sci.*, **55**, 15867 (2020).
11. I. Shitanda, K. Sugaya, C. Baba, N. Loew, Y. Yamagata, K. Miyamoto, S. Niinobe, K. Komatsuki, H. Watanabe, and M. Itagaki, "Rheo-Impedance Measurements for the Dispersibility Evaluation of Electrode Slurries." *ACS Applied Electronic Materials*, **5**, 4394 (2023).
12. DIN ISO 813:2020-12, (2020), Rubber, vulcanized or thermoplastic - determination of adhesion to a rigid substrate -90° peel method (ISO 813:2019), [10.31030/3205556](https://doi.org/10.31030/3205556).
13. M. Kosfeld, B. Westphal, and A. Kwade, "Correct water content measuring of lithium-ion battery components and the impact of calendaring via Karl-Fischer titration." *Journal of Energy Storage*, **51**, 104398 (2022).
14. A. Smith, P. Stüble, L. Leuthner, A. Hofmann, F. Jeschull, and L. Mereacre, "Potential and limitations of research battery cell types for electrochemical data acquisition." *Batteries & Supercaps*, **6**, e202300080 (2023).
15. N. O. Laschuk, E. B. Easton, and O. V. Zenkina, "Reducing the resistance for the use of electrochemical impedance spectroscopy analysis in materials chemistry." *RSC Adv.*, **11**, 27925 (2021).
16. C. G. Lopez, R. H. Colby, and J. T. Cabral, "Electrostatic and hydrophobic interactions in NaCMC aqueous solutions: effect of degree of substitution." *Macromolecules*, **51**, 3165 (2018).
17. C. G. Lopez, S. E. Rogers, R. H. Colby, P. Graham, and J. T. Cabral, "Structure of sodium carboxymethyl cellulose aqueous solutions: A SANS and rheology study." *J. Polym. Sci., Part B: Polym. Phys.*, **53**, 492 (2015).
18. K. Hofmann, A. D. Hegde, X. Liu-Theato, R. Gordon, A. Smith, and N. Willenbacher, "Effect of mechanical properties on processing behavior and electrochemical performance of aqueously processed graphite anodes for lithium-ion batteries." *J. Power Sources*, **593**, 233996 (2024).
19. J. H. Park, S. H. Kim, and K. H. Ahn, "Role of carboxymethyl cellulose binder and its effect on the preparation process of anode slurries for Li-ion batteries." *Colloids Surf., A*, **664**, 131130 (2023).
20. C. Dwivedi, T. R. Mohanty, S. D. Manjare, S. K. Rajan, S. Ramakrishnan, S. K. P. Amarnath, D. Lorenzetti, and P. K. Mohamed, "Application of non-ionic surfactant in modifying the surface of carbon black and its role in the formation of colloidal composite materials." *Colloids Surf., A*, **624**, 126825 (2021).
21. T. Liebert, S. Hornig, S. Hesse, and T. Heinze, *Macromol. Symp.*, **223**, 253 (2005).
22. S. Lim, K. H. Ahn, and M. Yamamura, "Latex migration in battery slurries during drying." *Langmuir*, **29**, 8233 (2013).
23. C. G. Lopez, "Entanglement of semiflexible polyelectrolytes: Crossover concentrations and entanglement density of sodium carboxymethyl cellulose." *J. Rheol.*, **64**, 191 (2020).
24. C. G. Lopez and W. Richtering, "Oscillatory rheology of carboxymethyl cellulose gels: influence of concentration and pH." *Carbohydrate Polym.*, **267**, 118117 (2021).
25. L. Xiquan, Q. Tingzhu, and Q. Shaoqi, "Kinetics of the carboxymethylation of cellulose in the isopropyl alcohol system." *Acta Polym.*, **41**, 220 (1990).
26. N. Keim, "The Critical Role of NaCMC on Electrode Properties and Cell Performance in Lithium-Ion Batteries." *Dissertation*, Karlsruhe Institute of Technology (2025), [10.5445/ir/1000182378](https://doi.org/10.5445/ir/1000182378).
27. S. Jaiser, J. Kumberg, J. Klaver, J. L. Urai, W. Schabel, J. Schmatz, and P. Scharfer, "Microstructure formation of lithium-ion battery electrodes during drying—an ex situ study using cryogenic broad ion beam slope-cutting and scanning electron microscopy (Cryo-BIB-SEM)." *J. Power Sources*, **345**, 97 (2017).
28. A. Weber, N. Keim, A. Gyulai, M. Müller, F. Colombo, W. Bauer, and H. Ehrenberg, "The role of surface free energy in binder distribution and adhesion strength of aqueously processed LiNi<sub>0.5</sub>Mn<sub>1.5</sub>O<sub>4</sub> cathodes." *J. Electrochem. Soc.*, **171**, 040523 (2024).
29. D. Yang, X. Li, N. Wu, and W. Tian, "Effect of moisture content on the electrochemical performance of LiNi<sub>1/3</sub>Co<sub>1/3</sub>Mn<sub>1/3</sub>O<sub>2</sub>/graphite battery." *Electrochim. Acta*, **188**, 611 (2016).